PHARMACEUTICAL NANOTECHNOLOGY

Studies on Binary Lipid Matrix Based Solid Lipid Nanoparticles of Repaglinide: *in Vitro* and *in Vivo* Evaluation

MANOJ K. RAWAT, ACHINT JAIN, SANJAY SINGH

Department of Pharmaceutics, Institute of Technology, Banaras Hindu University, Varanasi 221 005, India

Received 1 June 2010; revised 20 August 2010; accepted 18 November 2010

Published online 5 January 2011 in Wiley Online Library (wileyonlinelibrary.com). DOI 10.1002/jps.22435

ABSTRACT: The purpose of present study is to examine effect of binary lipid matrix (combination of lipids) on the entrapment and storage stability of repaglinide (RG) loaded solid lipid nanoparticles (SLN). Solid lipid nanoparticles were prepared by modified solvent injection method for oral delivery to improve the bioavailability of RG, an antidiabetic drug. The stearic acid and tristearin were used to form lipid core materials, and Pluronic-F68 was used as a stabilizer. Nanoparticles were characterized by evaluating their particle size, zeta potential, entrapment efficiency, drug loading, solid-state studies (differential scanning calorimetry, X-ray diffraction), *in vitro* drug release, particle surface (transmission electron microscopy analysis with electron diffraction pattern), stability study in gastrointestinal fluids (GIFs) and storage stability at 30°C/65% RH for 3 months. The characterization of SLN suggested that binary lipid matrix based nanoparticles had better drug entrapment and loading, desired release characteristics, stable in GIFs and significantly higher storage stability compared with single lipid formulations. Pharmacodynamic (blood glucose, blood cholesterol, blood triglyceride levels) and pharmacokinetic (AUC, T_{max}, peak plasma concentrations, K, $t_{1/2}$, mean residence time and relative bioavailabilities) studies were performed for the selected formulations. These studies indicate that the formulation based on binary lipid matrix significantly improves the oral bioavailability of RG. © 2011 Wiley-Liss, Inc. and the American Pharmacists Association J Pharm Sci 100:2366–2378, 2011

Keywords: Nanoparticles; lipids; first-pass metabolism; stability; bioavailability; morphology; particle size; biodegradable; oral absorption; intestinal lymphatic route

INTRODUCTION

Oral route is the most commonly used and preferred route of choice for the delivery of drugs, although several factors like pH of gastrointestinal tract, residence time, absorption and solubility can affect the bioavailability of drug by this route. Lymphatic delivery is an emerging way to avoid first pass metabolism in peroral drug delivery.[1] The conventional approaches such as use of permeation enhancers, surface modification, prodrug synthesis, complex formation and colloidal lipid carrier based strategies have been developed for the delivery of drugs to intestinal lymphatics.[2,3] In addition, polymeric nanoparticles, self-emulsifying delivery systems, liposomes, microemulsions, micellar solutions and recently solid lipid nanoparticles (SLN) have been exploited as probable possibilities as carriers for oral intestinal lymphatic delivery. Since 1991, SLN have been investigated comprehensively in drug delivery through various administration routes. The SLN-based systems possess characteristics of conventional carriers as well as some additional characteristics that prevent the drawbacks associated and reported for conventional systems. So, it has become an effective substitute for conventional system.[4–6] Solid lipid nanoparticles are also useful carriers for the successful delivery of peptides (insulin) and anticancer drugs (doxorubicin) through the oral intestinal route.[7,8] Solid lipid nanoparticles enhance lymphatic transport of the drugs, reduce the hepatic first-pass metabolism and improve bioavailability, because intestinal lymph vessels drain directly into the thoracic duct, further in to the venous blood, thus by passing the portal circulation.[5,9] Solid lipid nanoparticles are composed of a lipid core that may mimic chylomicrons formation, which ultimately takes the carrier

Correspondence to: Sanjay Singh (Telephone: +91-542-670-2712; Fax: +91-542-236-8428; E-mail: ssingh.phe@itbhu.ac.in, bitsmanoj@gmail.com)

Journal of Pharmaceutical Sciences, Vol. 100, 2366–2378 (2011)

along with the coentrapped drug by following the classical transcellular mechanism of lipid absorption.[10] Initially, Bargoni et al.[2] demonstrated the lymphatic uptake of SLN after oral administration at preclinical level. Luo et al.[11] reported that oral administration of vinpocetine-loaded SLN sustained release and improved bioavailability. Recently, Li et al.[12] also studied the pharmacokinetic aspects of quercetin-loaded SLN after oral administration and found that SLN improved the oral bioavailability.

Various lipids (matrix materials) used for the production of SLN are glyceride, fatty acid and hard fat or cetyl palmitate. The basic advantages of these systems include their biocompatibility, high drug pay load, easy scale up of production and physical stability.[13] However, despite the initial claims regarding their potential for the physical storage stability, so far, SLN have shown instability during storage, owing to the crystallinity and polymorphic behaviour of lipids.[14] These are the most important key factors, which have a direct impact on the entrapment efficiency (EE), drug loading (DL), physical stability and release kinetics. Hence, degree of crystallinity needs to be considered in selection of the lipids for formulation of SLN. Entrapment efficiency of the drug in the lipids depends upon the factors such as miscibility, solubility of drug in lipid melt, physical and chemical structure of the lipid matrix and polymorphic state of lipid materials.[15] Lipids that form highly crystalline particles with a perfect lattice (e.g., fatty acid) cause drug expulsion. More complex lipids (triglycerides) form less perfect crystals with many imperfections. These imperfections provide space to accommodate the drugs. Single lipid matrixes have perfect crystal lattice, which is responsible for drug expulsion and subsequently lower EE and physical instability.[16] On the other hand, binary lipid matrix can create deformation in crystal order of lipids and avoid the drug expulsion. The use of binary lipid matrix in fabrication of SLN has not received due attention by the researchers as yet. In order to improve the EE and physical stability of SLN, an attempt was made to develop the stearic-based binary SLN by the addition of titrated amount of tristearin. Repaglinide (RG) was selected as a model drug (oral hypoglycemic), which has poor oral bioavailability with short terminal elimination half-life because of the first-pass metabolism.[17] The prepared SLN were characterized for their particle size, polydispersity index (PDI), zeta potential, EE, DL, solid state studies (differential calorimeter and X-ray diffraction), stability in gastrointestinal fluids, physical stability at 30°C/65% RH for 3 months, *in vitro* drug release and surface structural analysis by transmission electron microscope. Furthermore, performed pharmacodynamic (blood glucose, blood cholesterol and blood triglyceride level) and pharmacokinetic [AUC, T_{max}, peak plasma concentrations (C_{max}), K, $t_{1/2}$, mean residence time (MRT) and relative bioavailabilities (% *Fr*)] studies of selected SLN formulations in STZ-induced diabetic rats to assess any enhancement in oral bioavailability of RG.

MATERIALS AND METHODS

Materials

Repaglinide and stearic acid (SA ≤98% purity) were a kind gift from Wockhardt Research Centre (Aurangabad, India). Tristearin (TS ≤ 99% purity) was purchased from Sigma–Aldrich (Lyon, France). Soya lecithin (≤ 97% purity) was purchased from Acros Organic (New Jersey, USA). Pluronic-F68 (PL-F68), sodium lauryl sulfate (SLS) and sodium carboxymethyl cellulose (NaCMC) were generously supplied by SRL (Mumbai, India). Dialysis membrane (molecular weight cutoff between 12,000–14,000 Da) was purchased from HiMedia (Mumbai, India). Glucose oxidase/Peroxidase kit (GOD/POD method), cholesterol kit (enzymatic CHOD-PAP method) and triglyceride liquid gold kit were purchased from Span Diagnostic Ltd. (Surat, India). The all other chemicals were of analytical and high-performance liquid chromatography (HPLC) grade. In this study, purified water from Direct Q® 3 UV system of Millipore having the pH 6.65 ± 0.40 was used.

Preparation of SLN

Stearic acid, TS and soya lecithin [0.04% (w/v)] along with RG [0.02% (w/v)] were dissolved in 2 mL of dichloromethane. Thereafter, immediately injected (1 mL/min) through an injection needle (0.45 mm syringe diameter) into the 100 mL aqueous phase containing 0.25 g of PL-F68 (stabilizer) under continuous stirring (2000 rpm for 2 h: Ika, Germany) at room temperature. Dichloromethane and some proportion of water were eliminated at 40°C under reduced pressure by using vacuum oven (Decibel, Digital Technologies, India) and the final volume of the aqueous nanosuspension was adjusted to 20 mL.

Repaglinide-loaded SLN obtained using SA and in combination with partial amount of TS (binary lipid matrix) were abbreviated as RSA (SA:TS, 100:0), RST_{10} (SA:TS, 90:10), RST_{20} (SA:TS, 80:20) and RST_{30} (SA:TS, 70:30), respectively. Formulae of all the prepared formulations are shown in Table 1.

Particle Size and Zeta Potential Analysis

The particle size was measured by dynamic light scattering (Nano ZS, Malvern Instruments), and zeta potential was estimated on the basis of electrophoretic mobility under an electric field. In order to analyze the particle size, nanosuspensions were diluted five times with purified water.

Table 1. Composition of Solid Lipid Nanoparticles for Different Formulations

Ingredients	RSA	RST_{10}	RST_{20}	RST_{30}
Repaglinide (mg)	20	20	20	20
Stearic acid (mg)	200	180	160	140
Tristearin (mg)	–	20	40	60
Lecithin (mg)	40	40	40	40
Pluronic F68 (mg)	250	250	250	250

Purified water (q.s. for 100 mL)

HPLC Analytical Method

High-performance liquid chromatography analytical method was developed for estimation of total drug content (TDC), EE, DL and *in vitro* drug release of RG–SLN. The analytical method used was a reversed-phase HPLC (Cecil CE4201, India) in a binary mode (dual pump), with a ultraviolet (UV) detector at 282 nm. The HPLC column was Phenomenex ($C_1$8 reverse phase, 250 mm × 4.5 mm, 5 µ column). The mobile phase of acetonitrile–ammonium formate (pH 2.7; 0.01 mM) [60:40% (v/v)] delivered with a flow rate of 1 mL/min.The retention time of the drug was found to be 4.51 ± 0.1 min.

The validation parameters for the developed *analytical* method were as accuracy [% recovery ± standard deviation (SD)]: 101.024 ± 2.10, precision (% CV ± SD): intra-day: 1.10 ± 0.68; inter-day: 1.71 ± 0.94, linearity : 2–10 µg/mL, LOD : 0.60 µg/mL, LOQ : 1.50 µg/mL.

Determination of TDC

Nanosuspension (1 mL) were diluted to 10 mL with chloroform:methanol mixture (1:2) and filtered by a 0.45-µm filter paper, and TDC was determined by HPLC (Cecil CE4201, India) as described above.

Determination of EE and DL

The EE and DL in nanosuspension were calculated as described by Muthu and Singh.[18] Free dissolved drug amount present in the nanosuspension was determined by bulk equilibrium reverse dialysis bag technique. Briefly, a dialysis bag (cellulose membrane, molecular weight cut-off 12,000 Da) containing 1 mL of distilled water with 25 mg PL-F68 was placed directly into 10 mL of nanosuspension. After equilibrium (8 h), dialysis bag was withdrawn from the nanosuspension. The sample collected from the dialysis bag was assayed by the HPLC method as described above.

The calculation was performed as follows:

$$Free\ dissolved\ drug = \frac{Total\ volume}{volume\ of\ \ dialysis\ bag} \times Drug\ amount\ in\ the\ dialysis\ bag$$

where total volume is the sum of total volume of the nanosuspension and volume of the dialysis bag sample.

$$EE\,(\%) = \frac{Total\ Drug\ Content - Free\ dissolved\ drug}{Drug\ amount\ used} \times 100$$

$$\%\,DL = \frac{Total\ Drug\ Content - Free\ dissolved\ drug}{Drug\ amount\ used - Free\ dissolved\ drug + Wight\ of\ \ the\ lipid} \times 100$$

Solid State Characterization

Characterization by Differential Scanning Calorimeter

Thermograms of the different samples (RG, SA, TS and lyophilized SLN (RST, RST_{10}, RST_{20} and RST_{30}) were obtained from a DSC (DSC 30; Mettler–Toledo, Viroflay, France). Lyophilized SLN samples (3–5 mg) were heated in sealed standard aluminum pans from 0 to 160°C at a scanning rate of 10°C/min under nitrogen purge, with an empty aluminum pan as reference.

Characterization by X-Ray Diffractometer

X-ray diffractometer (Siemen's D-5000, Germany) was used for diffraction studies. X-ray diffractometer studies were performed on the samples by exposing them to Cu–K radiation (40 kV, 30 mA) and scanned from 5° to 80°, 2θ at a step size of 0.045° and step time of 0.5 s. Samples used for XRD analysis were RG, SA, TS, lyophilized SLN (RSA, RST_{10}, RST_{20} and RST_{30}).

Stability Studies in Gastrointestinal Fluids

Stability studies were carried out in order to investigate the particle aggregation in simulated gastric fluid (SGF) and simulated intestinal fluid (SIF). The SGF and SIF were prepared according to the USP XXIV (US. Pharmacopeia. XXIV, 2006).[19] The SGF medium contained 0.32% (w/v) of pepsin; the pH was 1.2. The SIF medium was composed of 1% (w/v) pancreatin with a pH of 7.5.

Different formulations incubated at 37°C in SGF and SIF. Samples were collected at times 0 h (before addition to SGF and SIF) and 3 h for investigation of particle size and its distribution pattern (PDI).

Stability Studies at 30°C/65% RH

To investigate the physical stability of the RG–SLN on storage, samples were stored for 3 months at 30°C/65% RH (Labtop stability chamber; Skylab Instrument & Engineering Pvt Ltd, Mumbai, India) and characterized for particle size, PDI and EE.

Determination of Saturation Solubility of RG in Dissolution Medium

Repaglinide saturation solubility (Cs) was obtained by dispersing 300 mg drug in 50 mL of phosphate

buffer pH 6.8 containing 0.5% SLS. The suspension was stirred under constant magnetic stirring (100 rpm) at 37 ± 0.5°C for 24 h (sufficient time for equilibration), filtered through a syringe filter (0.45 μm) and then assayed by the HPLC (Cecil CE4201, India) method as described above. The experimental values were the average of three replicates ($n = 3$).

In Vitro Release Study

In vitro release studies were performed using the dialysis bag diffusion technique.[20,21,22] Dialysis membrane (molecular weight, 12,000 Da) was soaked in double-distilled water for 12 h before use for experiment. Repaglinide aqueous nanosuspension or control (RG suspension in 0.5% NaCMC) equivalent to 5 mg of RG was placed in the dialysis bag containing 50 mL of dissolution medium [phosphate buffer pH 6.8 containing 0.5% (w/v) SLS] at 37 ± 0.5°C with continuous magnetic stirring at 200 rpm. At fixed time intervals, the samples were withdrawn; same dissolution media was replaced by fresh medium to maintain constant volume. Sink conditions were maintained for release studies ($C_1 < Cs \times 0.2$),[23] where C_1 is the final concentration of RG after the complete release of the drug in dissolution medium and Cs is the saturation solubility of RG in the dissolution medium. Samples were analyzed by the HPLC method as described above.

Aqueous suspension of RG in 0.5% (w/v) NaCMC was used as control for the *in vitro* release studies.

Surface Structural Analysis

The external morphology and electron diffraction (ED) pattern of nanoparticles were determined by transmission electron microscopy (TEM) (TECNAI-12; FEI, Eindhoven, the Netherlands). The samples were stained with 2% (w/v) phosphotungstic acid and placed on copper grids with films to view by TEM.

Animal Study Protocol

The study protocol was approved by the Animal Ethical Committee, Institute of Medical Science, Banaras Hindu University, Varanasi, India. The male Wistar rats were quarantined in the animal house maintained at 20 ± 2°C and 50%–60% RH. A 12-h dark/light cycle was maintained throughout the study. Rats had free access to food (pellet diet supplied) and distilled water *ad libitum*. Thirty male rats weighing 170 ± 20 g were kept for overnight fasting. Animals were divided into five groups comprising six animals in each group ($n = 6$). The animals of group I served as control, whereas group II served as diabetic control. All the animals of group III were given an oral dose of RG suspension; group IV was administered with RSA formulation orally, and group V was given optimized batch of binary SLN in equivalent doses of RG orally.

Pharmacodynamic and Pharmacokinetic Study

Diabetes was induced in the rats using streptozotocin (STZ) equivalent to 65 mg/kg body weight. Streptozotocin was dissolved in 0.5 mL citrate buffer (pH 4.5) and administered intraperitoneally to the rats.[24] After 7 days, the extent of diabetic induction was monitored based on blood-sugar level and a decrease in weight. Blood glucose (BG) levels of at least 350 mg/dL were accepted as the basal level for diabetes. The rats were fasted for 18 h, and the RG suspension [RG aqueous suspension in 0.5% (w/v) NaCMC] or optimized batches of RG–SLN (0.286 mg/kg) were administered to the rats using gavage. Six diabetic rats were used in each group. Blood samples (0.5 mL) were collected from the retro orbital vein in heparin-coated Eppendorf tubes at 1, 2, 4, 8, 16 and 24 h after drug administration.[25] The blood samples were centrifuged at 2347× g (rpm: 5000 and radius: 8.39 cm) for 5 min. Plasma was collected and stored at –40°C until analyze for BG, BC and BT levels. The areas under the effect versus time (AUEC) and Nadir effect (maximum BG lowering effect) were calculated as pharmacodynamic parameters. The parameters such as C_{max}, T_{max}, AUC, K, $t_{1/2}$, MRT and % Fr were determined in pharmacokinetic analysis.

HPLC Bioanalytical Method

High-performance liquid chromatography bioanalytical method was developed for estimation of RG in plasma. The bioanalytical method used was a reversed-phase HPLC (Cecil CE4201, India) in a binary mode (dual pump), with a ultraviolet (UV) detector at 282 nm. The HPLC column was Phenomenex (C18 reverse phase, 250 mm × 4.5 mm, 5 μ column). The mobile phase of acetonitrile–ammonium formate (pH 2.7; 0.01 mM) [60:40% (v/v)] delivered with a flow rate of 1 mL/min.The retention time of the drug was found to be 4.52 ± 0.05 min.

The validation parameters for the developed bioanalytical method were as accuracy [% recovery ± standard deviation (SD)]: 101.84 ± 1.29 , precision (% CV ± SD): intra-day: 1.72 ± 0.78 ; inter-day: 2.06 ± 0.98, linearity : 2–12 ng/mL, LOD: 1.12 ng/mL, LOQ : 2.00 ng/mL.

Plasma Sample Preparation

Liquid–liquid extraction method was used for the determination of RG in human plasma. The 1-mL RG solution (2, 4, 8, 10 and 12 ng/mL) was added to blank plasma samples (150 μL) in centrifuge tube. One millilitre extraction buffer (0.1 M KH_2PO_4, pH 5.9) was added to the tubes. The mixture was vortexed, 5 mL ethylacetate (recovery solvent) and 50 μL isoamylalcohol were added and the pH adjusted to 7.4 with 2 M NaOH. The tubes were shaken manually

for 10 min. This was followed by centrifugation at 2347× *g* for 5 min. After centrifugation, the ethyl acetate phase was transferred into another centrifuge tubes and evaporated to dryness in vacuum oven on 400-mmHg pressure at 45°C. The dried extract was reconstituted with 40 μL of mobile phase. Twenty microlitres of this solution was injected into the HPLC system.

Pharmacodynamic Analysis

The BG, blood cholesterol (BC) and blood triglycerides (BT) level were analysed by using glucose oxidase kit (GOD/POD method), cholesterol kit (enzymatic CHOD-PAP method) and triglyceride liquid gold kit, respectively.[26] The areas under the effect versus time and Nadir effect were the best approach for measuring the antidiabetic efficacy. The areas under the effect versus time were determined from graphical plots of % BG (the percentage was calculated based on the values for normal saline as the baseline) versus time (h). The Nadir effect is the percentage of maximum lowering of the glucose level at time t (t_{Nadir}) with respect to the percentage of the basal BG level.[27]

Pharmacokinetic Analysis

Non-compartmental analysis with WinNonlin software (Version 4.1) was used to estimate the pharmacokinetic parameters ($C_{\max}$, $T_{\max}$, $\text{AUC}_{0-\infty}$, K, $t_{1/2}$ and MRT) of RG. Relative bioavailability (% *Fr*) of SLN formulations was calculated by using the following formula:

$$\%\,Fr = \text{AUC}_{\text{SLN}}/\text{AUC}_{\text{suspension}} \times 100$$

Statistical Analysis

The results were expressed as mean values ± SD. The analysis of variance was applied to examine the significance of differences between batches of nanoparticles' properties (such as particle size, zeta potential, EE, TDC, *in vitro* release studies and pharmacokinetic study). The analysis of variance followed by a *post hoc Tukey multiple comparison test* was performed for comparison in pharmacological evaluation of treatments. In all cases, $p < 0.05$ was considered to be significant.

RESULTS AND DISCUSSION

Measurement of Size, TDC and EE

Particle sizes, polydispersity index (PDI), zeta potential, TDC and EE of RG–SLN with different formulation batches are shown in Table 2. In all formulations, particle sizes and PDI are ranged from 175 to 350 nm and 0.120 to 0.320 nm, respectively, which shows the narrow particle size distribution. The particle sizes of RST_{30} (70:30) were smaller than those of RST_{10} (90:10), RST_{20} (80:20). The increasing of TS content in SLN formulations could reduce the melting point of SA lipid matrix and crystal order disturbance in lipid matrix, leading to favour the formation of SLN with smaller particle size. Zeta potential is a key factor to evaluate the stability of colloidal dispersion. High potential values should be achieved to ensure high-energy barrier and also favour good stability. Highly charged nanoparticles are better stable as colloidal suspensions because the Coulombic repulsion forces arising from their surface charge can overcome the Van der Waals attractive forces between them and prevent aggregation on ageing.[18] The zeta potential of the studied formulations varied from -23.10 ± 2.13 to -25.04 ± 1.99 mV, which is nearer to −25 mV of ideal stabilization.[28] No significant ($p > 0.05$) difference in the zeta potential of nanoparticles was observed in the case of all formulations. Total drug content for all the prepared formulations was nearer to 98%. Formulation RSA has shown significantly less drug EE compared with those of RST_{10}, RST_{20} and RST_{30} (binary lipid matrix based SLN) ($p < 0.05$). The EE of the RG–SLN were in the order of RSA (52.03 ± 1.29) < RST_{10} (60.14 ± 1.29) < RST_{20} (72.14 ± 1.29) < RST_{30} (81.40 ± 2.40). The DL of the RG–SLN were in the order of RSA (4.75 ± 0.30) < RST_{10} (5.58 ± 0.20) < RST_{20} (6.68 ± 0.51) < RST_{30} (7.45 ± 0.41). The higher EE and DL with the binary lipid matrix based SLN (RST_{30}) are attributed to the deformation of the crystal lattice of the SA lipid by TS lipid as well as an increase in the solubility of RG in lipid matrix.[14,29] By adding the TS to the SA carrier, the EE and DL were increased in a concentration-dependent manner. Entrapment efficiency of the drug in the lipids depends upon the factors such as miscibility, solubility of drug in lipid melt, physical and chemical structure

Table 2. Characteristics of SLN for Different Formulations

Batch Code	Size (nm)	PDI	Zeta Potential (mV)	Total Drug Content (TDC) (%)	Entrapment Efficiency (EE) (%)	Drug Loading (DL) (%)
RSA	350 ± 4.3	0.320 ± 0.004	-23.10 ± 2.13	98.89 ± 1.06	52.03 ± 1.29	4.95 ± 0.30
RST_{10}	280 ± 2.6	0.148 ± 0.020	-24.53 ± 1.80	99.13 ± 2.33	60.14 ± 1.69	5.67 ± 0.20
RST_{20}	220 ± 2.39	0.134 ± 0.050	-24.25 ± 1.70	99.50 ± 2.89	72.14 ± 1.36	6.72 ± 0.51
RST_{30}	175 ± 2.19	0.120 ± 0.060	-25.04 ± 1.99	99.28 ± 1.89	81.40 ± 2.40	7.53 ± 0.41

Mean values ± SD of $n = 3$.

of the lipid matrix and crystalline state of lipid materials.[14] Lipids that form highly crystalline particles with a perfect lattice (e.g., SA) cause drug expulsion. More complex lipids (mixtures of mono-, di- and triglycerides containing fatty acids of different chain lengths) form less perfect crystals with many imperfections. These imperfections provide space to accommodate the drugs.

Solid-State Characterization

Differential scanning calorimeter gives an insight into the melting and recrystallization behaviour of crystalline material like SLN. The breakdown of the crystal lattice by heating the sample yields inside information on, for example polymorphism, crystal ordering, eutectic mixtures or glass transition processes.[30] Differential scanning calorimeter experiments are useful to understand solid dispersions such as solid solutions, simple eutectic mixtures or, as in this case, effect of TS lipid on crystal ordering of SA lipid. Figure 1 (a, b, c, d, e, f and g) gives an overview of the melting process of a RG–SLN. Figure 1a represents the melting point peak of RG at 135°C, which confirmed a crystalline structure. Nanoparticles were prepared with different ratios of SA to TS lipids combination (SA:TS 100:0. 90:10, 80:20 and 70:30). Figure 1d represents SA made SLN by using the modified solvent injection technique containing 0.2% (w/v) SA (SA:TS 100:0). Figures 1e–1g are recorded on lipid carriers with increasing TS amounts (RST_{10}, RST_{20} and RST_{30}). For the RSA, the melting process takes place with maximum temperature at 54.8°C (peak maximum). By adding the TS to the SA carrier, the melting point is depressed in a concentration-dependent manner. At 90:10, 80:20 and 70:30 lipid ratios, the melting points are depressed in following manners: 49.08, 45.2 and 41.12°C, respectively. Such a phenomenon was attributed to the small size of the nanoparticles and their high specific surface area, which can reduce their melting point by several degrees.[29] Apart from this, the presence of guest molecules in the lipid matrix also influences its crystallization degree and the lipid layer organization.[31]

The XRD pattern of RG, SA and TS shows a principal peak at 2θ angle of 7.65°, 21.38° and 25.23°, respectively (Figs. 2a–2c). The principal peak of RG was not reduced significantly in SA prepared RG–SLN (Fig. 2d), but it reduced significantly in SLN prepared with binary lipid matrix (peak disappeared in RST_{30}) (Figs. 2e–2g). This may be attributed to the incorporation of TS into the crystal lattice of the SA lipid, leading to a change in the crystallinity of the SA prepared RG–SLN. These values clearly indicate the possible changes in crystallinity of the lipid after TS lipid incorporation in SA prepared RG–SLN.

Stability Studies in GIFs

After addition of SLN batches to the gastrointestinal fluids (GIFs), the GIT stability of the samples was investigated by observing potential changes in PDI. It is evident from Table 3 that the SLN formulations were considered as physically stable as no distinctive

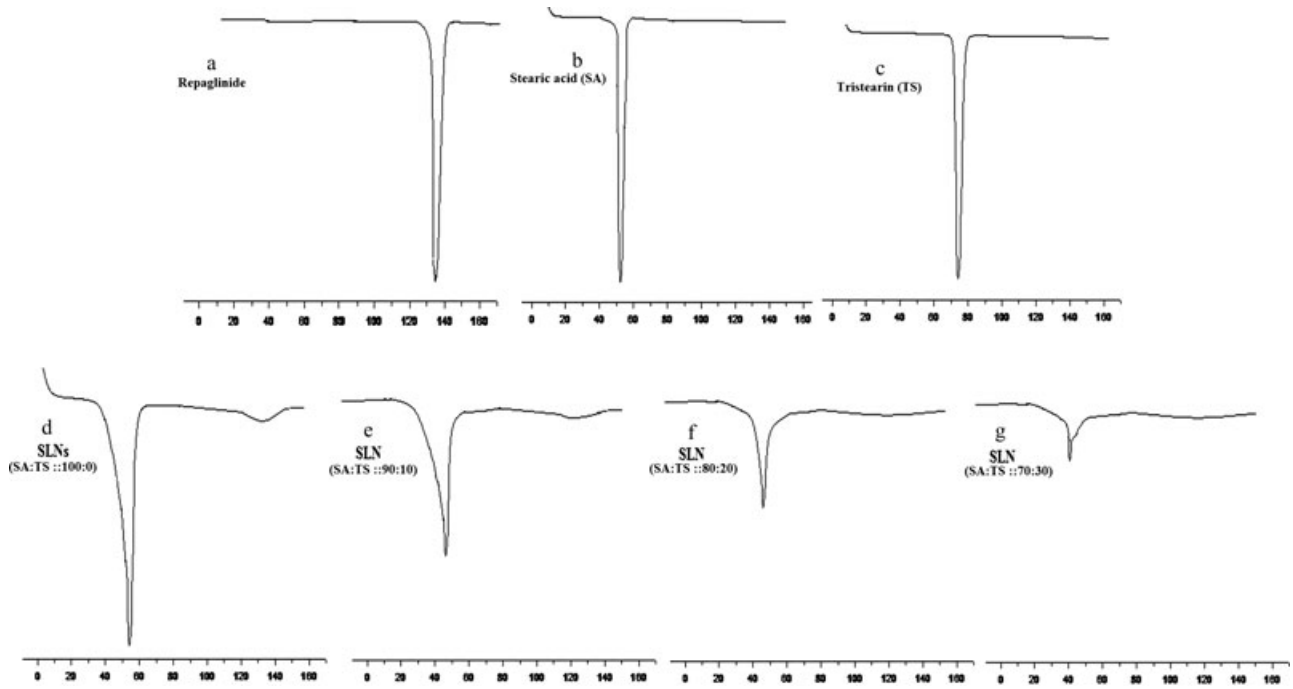

Figure 1. Differential scanning calorimeter thermograms: Repaglinide (a), stearic acid (b), tristearin (c), RSA (d), RST_{10} (e), RST_{20} (f), RST_{30} (g).

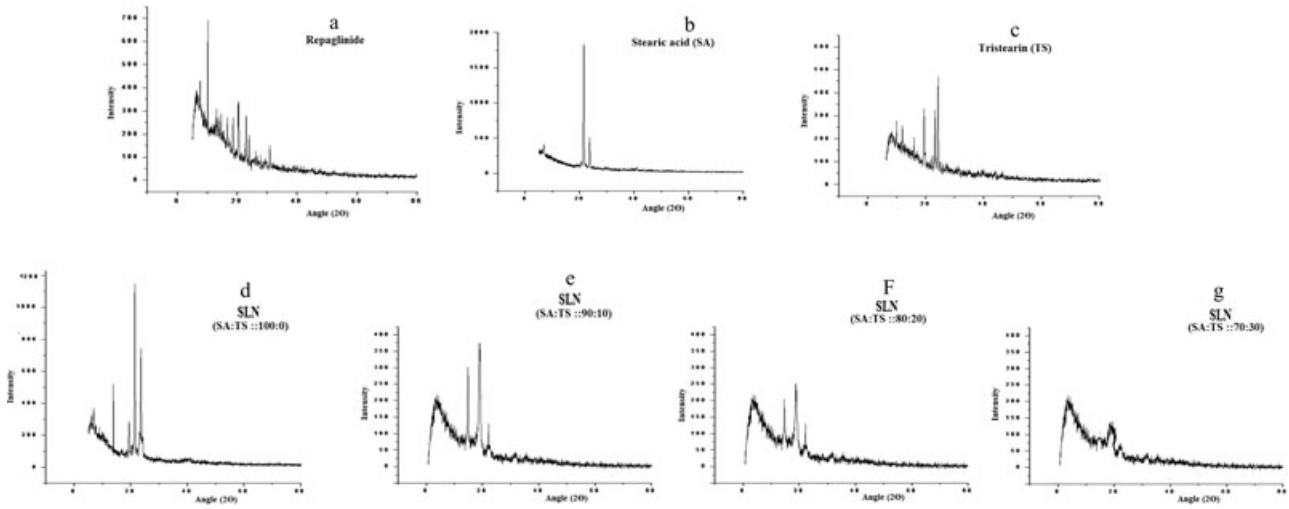

Figure 2. X-ray diffractometer patterns: Repaglinide (a), stearic acid (b), tristearin (c), RSA (d), RST_{10} (e), RST_{20} (f), RST_{30} (g).

aggregation or particle growth in the nanosuspension was detected at the end of 3 h. This may be attributed to the presence of protective coating of PL-F68 on the surface of SLN. In addition, PL-F68 gives the steric stabilization effect as it is a non-ionic surfactant. Similar results were obtained by Olbrich and Muller,[32] and Garcia–Fuentes et al.[33]

Stability Studies at 30°C/65% Rh

Storage at 30°C/65% RH for 3 months resulted in an increase in the particle size and PDI in all SLN. An increase in the particle size was in the order of RSA (370 ± 4.3 nm) > RST_{10} (295 ± 2.6 nm) > RST_{20} (210 ± 2.39 nm) > RST_{30} (178 ± 2.19). However, SLN prepared in RST_{30} batch were of lowest particle size increase ($p > 0.05$). Solid lipid nanoparticles prepared with binary lipid matrix (RST_{30}) exhibited good long-term stability, whereas SLN with fatty acid (SA) alone showed an increase in the particle size and particle agglomeration (an increase in PDI). An insignificant increase in PDI was observed in all batches except RSA (Table 4). The EE of all the batches (10.78% in RSA, 7.01% in RST_{10}, 6.65% in RST_{20} and 2.11% in RST_{30}) was decreased after storage at 30°C/65% RH for 3 months. However, the decrease was minimum in RST_{30} batch. The degree of crystallinity of SA lipid was responsible for destabilization of the SLN formulation. Stearic acid forms highly crystalline particles with a perfect crystal lattice that causes drug expulsion.[35] Because of this, EE was found to be decreased on storage. The higher ratio of TS in the SA lipid was responsible for better stability of RST_{30}. The highly disordered state in SA-prepared nanoparticles with a higher amount of TS delays recrystallization and thus improves physical stability.[35] RST_{30} batch was with the smallest particle size, highest EE and good long-term stability. Therefore, from binary lipid matrix based SLN, RST_{30} batch was selected for further studies.

Saturation Solubility and *In Vitro* Release Studies

The Cs of RG in phosphate buffer pH 6.8 containing 0.5% SLS was 610.5 µg/mL at 37 ± 0.5°C. Sink conditions were maintained for release study: $C_1 < Cs \times 0.2$.[23] C_1 was the final concentration of RG in medium after complete release of the drug in the phosphate buffer pH 6.8, containing 0.5% SLS. Therefore, the final concentration of RG after the complete release in dissolution media was maintained below 122.1 µg/mL, in compliance with the sink conditions.

Figure 3 shows the cumulative percentage release of drug from control RG suspension, RSA and RST_{30}

Table 3. Particle Size and PDI of Different Batches of Prepared SLN Formulations Before Addition (= Original SLN) and After Addition to the Gastrointestinal Fluids After 3 h Incubation

	Original SLN		Simulated Gastric Fluid (SGF)		Simulated Intestinal Fluid (SIF)	
Batch Number	Size (nm)	PDI	Size	PDI	Size	PDI
RSA	347 ± 3.90	0.320 ± 0.004	348 ± 2.51	0.331 ± 0.014	351 ± 3.22	0.325 ± 0.010
RST_{10}	278 ± 2.82	0.148 ± 0.020	283 ± 1.99	0.137 ± 0.017	285 ± 2.14	0.142 ± 0.019
RST_{20}	221 ± 2.30	0.134 ± 0.050	216 ± 1.79	0.129 ± 0.026	223 ± 1.80	0.139 ± 0.020
RST_{30}	177 ± 2.41	0.120 ± 0.060	173 ± 2.01	0.116 ± 0.041	179 ± 2.29	0.123 ± 0.014

Mean values ± SD of $n = 3$.

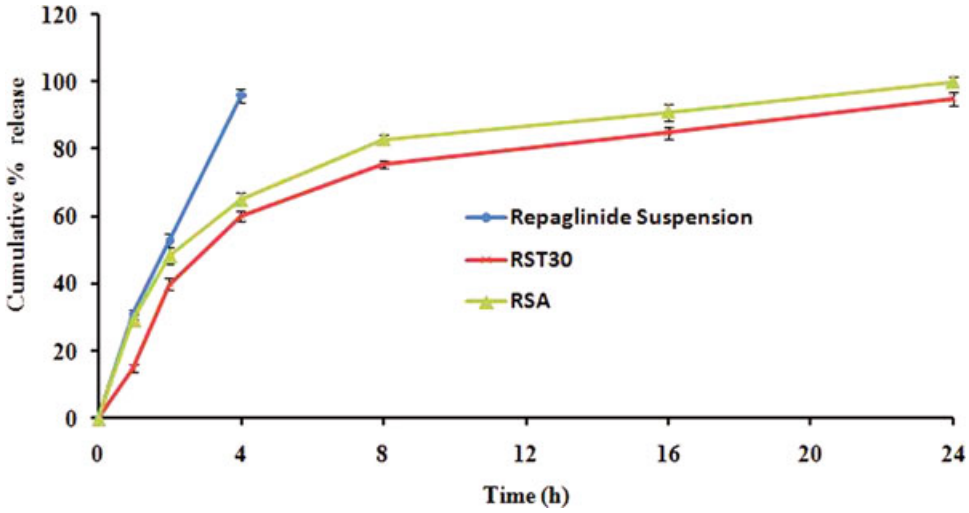

Figure 3. *In vitro* release of repaglinide (RG) from repaglinide suspension and RG–SLN.

batches. Complete RG release (100%) was achieved within 8 h from the control RG suspension across the dialysis bag, which indicates rapid diffusion of the RG. In the case of the control RG suspension, the time required for 50% drug release ($T_{50\%}$) was 1.5 h whereas for SLN it was 2.33 h (RSA) and 3.45 h (RST_{30}). The prolonged drug release was observed in RST_{30} batches as compared with RSA. The release of a drug from the SLN can be influenced by the nature of the lipid matrix, surfactant concentration and production parameters.[36] Because the surfactant concentration was constant, the drug release profile was affected by other parameters such as lipid nature, solubility of the drug in lipid and partition coefficient.[37,38] This clearly confirmed from the release profiles that the lipid concentration in the formulation is sufficient to prolong the drug release for longer period of time (Fig. 3).

Surface Structural Analysis

The colloidal solution of SLN prepared was milk white in physical appearance. The external morphological study using TEM revealed that all nanoparticles were spherical in shape (Figs. 4a and 4b). Solid lipid nanoparticles shape may mainly be decided by the property of lipid including solubility, crystal lattice and film-forming capability.[39] The nanoparticles size, as observed by TEM, correlated well with the size measured by Malvern zetasizer.

Electron diffraction of the drug-loaded (RST_{30}) and placebo (without drug) nanoparticles in TEM revealed the crystalline state of the SLN (Figs. 5a and 5b). These images clearly demonstrate that ring patterns in the electron diffraction were reduced in drug-loaded nanoparticles owing to the presence of amorphous RG.[18] This study confirmed that RG was well incorporated into the core of SLN (Fig. 5b). The presence of amorphous RG was also revealed in DSC and XRD studies.

Pharmacodynamic and Pharmacokinetic Studies

Figures 6, 7 and 8 show the BG, BC and BT levels, respectively, at different time intervals following oral administration of RG–SLN (RSA and RST_{30}) and RG suspension at a dose of 0.286 mg/kg to diabetic rats. From Figures 6–8, it is clear that the administration of RG–SLN had significant influenceinfluence on the BG, BC and BT levels compared with RG suspension ($p < 0.05$). In STZ-induced diabetic rats, the maximal effect was registered 0.3 h after treatment with the RG suspension and 4 h after treatment with RG–SLN. The AUEC obtained for RSA and RST_{30} were 1233.201 ± 2.6% and 1476.98 ± 3.98% h, respectively, whereas 49.409 ± 3.45% h for RG suspension (Table 5). The RST_{30} and RSA showed a greater

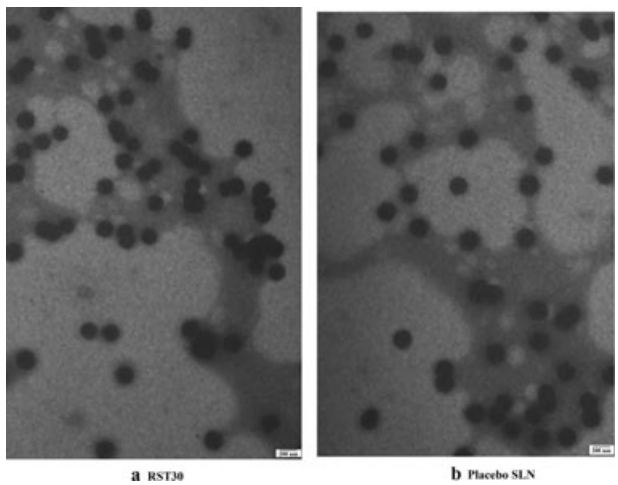

Figure 4. Transmitted electron micrographs of RST_{30} and placebo SLN.

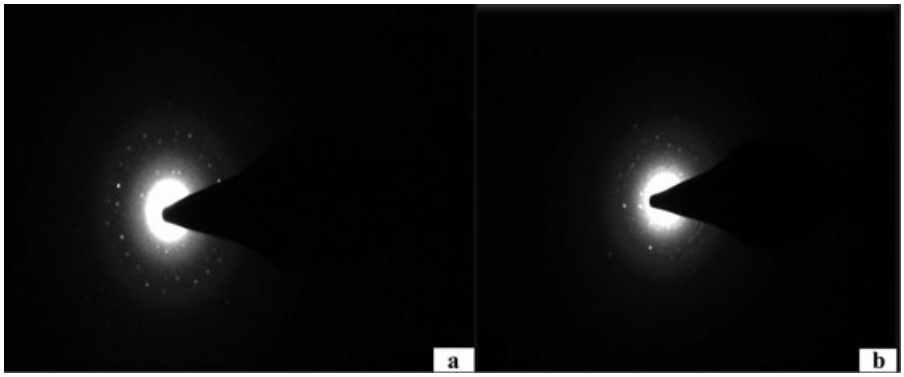

Figure 5. Electron diffraction ring pattern for RST_{30} and placebo SLN.

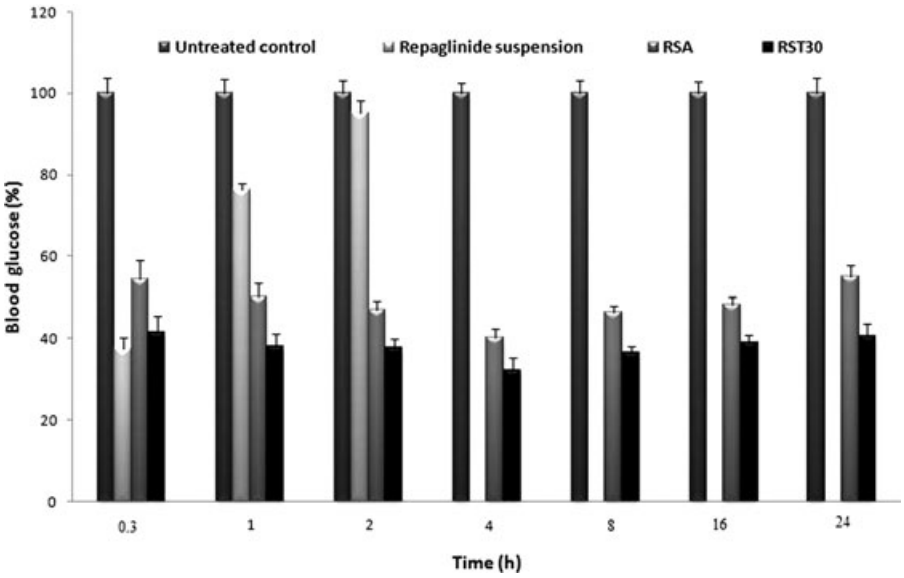

Figure 6. Blood glucose level of rats given repaglinide suspension and RG–SLN ($n = 6$).

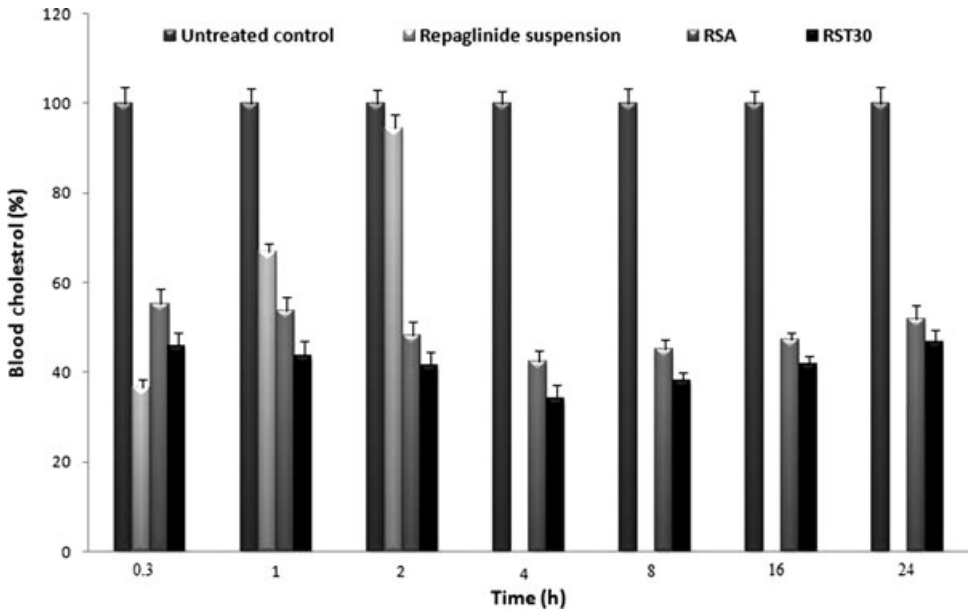

Figure 7. Blood cholesterol level of rats given repaglinide suspension and RG–SLN ($n = 6$).

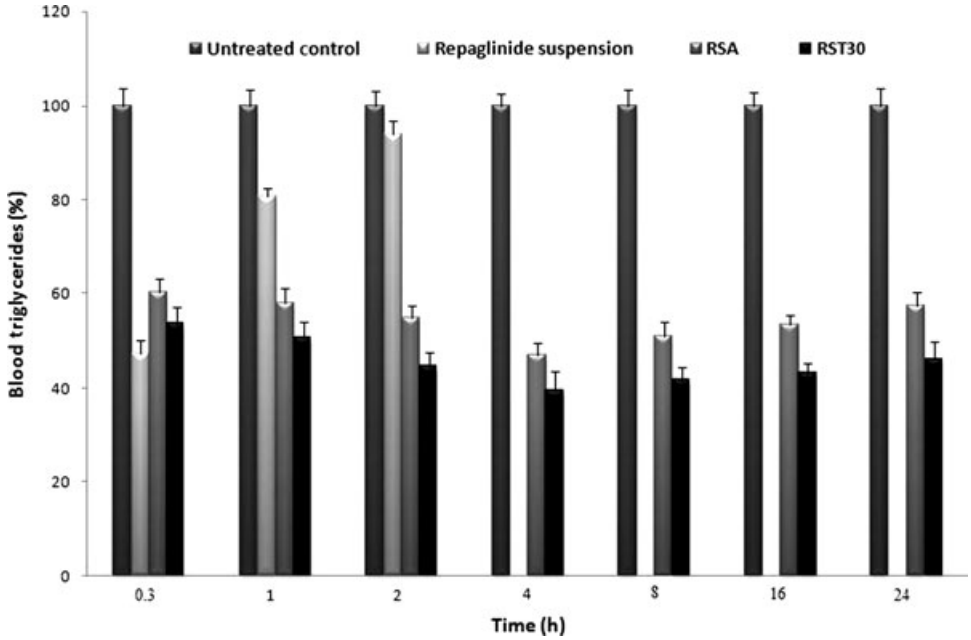

Figure 8. Blood triglyceride level of rats given repaglinide suspension and RG–SLN ($n = 6$).

antidiabetic effect for a longer period of time (in terms of basal reduction in the BG level) than RG. After the oral administration, the t_{Nadir} for RG suspension was 0.3 h and for RSA and RST_{30} batches it was 4 h (Table 5). The Nadir effect was observed for RG suspension, RSA and RST_{30} were $62.53 \pm 2.19\%$, $59.66 \pm 3.85\%$ and $67.82 \pm 2.14\%$, respectively. Figures 6 clearly indicate that RG–SLN can also reduce the blood lipid profiles for prolong period of time in diabetes-induced rats in comparison with the RG suspension ($p < 0.05$). This suggests that RG–SLN were more effective than RG in lowering glucose levels and also sustaining the drug release for a longer period of time.

The formulations RSA and RST_{30} were also evaluated for its oral bioavailability in diabetic rats to ascertain the pharmacokinetic parameters (AUC, T_{max}, C_{max}, K, $t_{1/2}$, MRT and $\%F$). A plasma concentration—time curve of RG and RG–SLN after oral administration is shown in Figure 9. Peak plasma concentrations were in the following order: RST_{30} (8.81 ± 0.089 ng/mL) > RSA (9.65 ± 0.045 ng/mL) > RG suspension (8.50 ± 0.01 ng/mL). T_{max} values are same (4 h) for

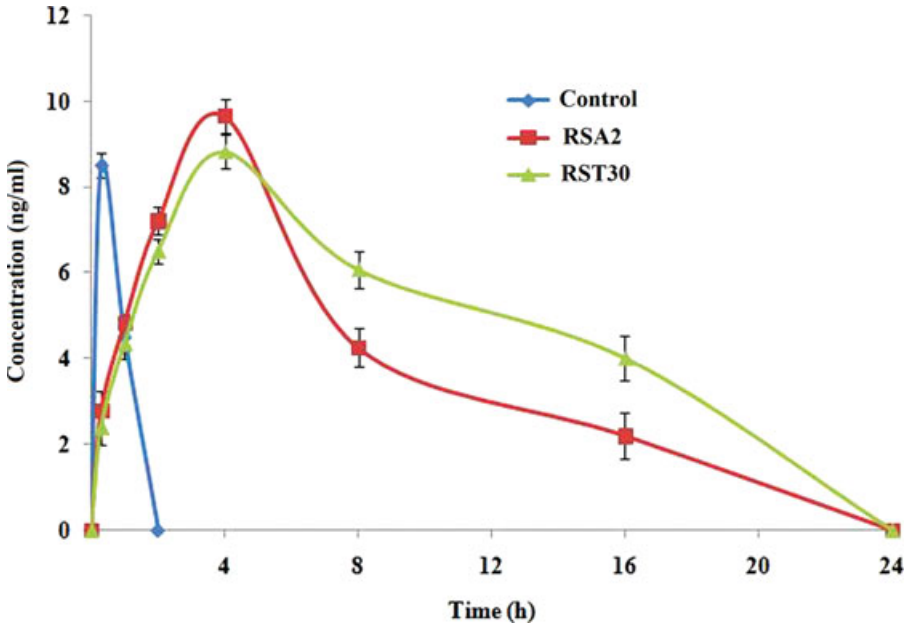

Figure 9. Mean plasma concentration of repaglinide (RG)–time curves after oral administration of repaglinide suspension and RG–SLN ($n = 6$).

Table 4. Effects of Storage Condition on Particle Size, PDI and EE of Optimized SLN Formulations

Parameters	RSA	RST_{10}	RST_{20}	RST_{30}
Particle size (nm)	370 ± 4.3	295 ± 2.52	210 ± 2.39	178 ± 2.09
PDI	0.570 ± 0.030	0.155 ± 0.022	0.139 ± 0.091	0.129 ± 0.029
Entrapment efficiency (EE) (%)	41.25 ± 1.32	53.13 ± 1.64	65.49 ± 1.19	79.29 ± 1.95

Mean values ± SD of $n = 3$.

RSA and RST_{30} but for RG suspension it was 0.3 h. The AUC of the SLN (RSA: 88.37 ± 2.01 and RST_{30}: 109.57 ± 3.01 h × ng/mL) was significantly ($p < 0.05$) higher than that of RG suspension (8.08 ± 1.98 h × ng/mL). Relative bioavailabilities were in the following order: RST_{30} (1356.06) > RSA (1093.69) > RG suspension (100). An increase in AUC and *% Fr* for SLN indicates that RG oral absorption was enhanced significantly compared with the RG suspension. The mean residence time of RST_{30} was also increased significantly ($p < 0.05$) when compared with RSA and RG suspension (Table 6). This may be attributed to the presence of a long chain fatty acid (TS) along with SA in RST_{30}. Longer $t_{1/2}$, increased T_{max} and MRT of RST_{30} as compared with RSA and RG suspension (Table 5) reiterate the *in vitro* results of prolonged release from the RST_{30} formulation. An increase in AUC and *% Fr* for SLN may be due to the avoidance of first-pass metabolism by lymphatic transport as first-pass metabolism was responsible for poor bioavailability of RG.[40,41] Previously, there are certain reports which show that lipid nature, fatty acid chain length and hydrophobicity will influence the lymphatic uptake.[20,42,43] Esterification of long-chain triglyceride (TS) formed surface active mono- and diacylglycerols, which can solubilize RG and subsequently, an interaction with bile salts takes place, leading to the formation of mixed micelles, which promote RG absorption.[44] This result indicated that oral absorption of RG was more in the case of RST_{30}. The EE, physical stability, *in vitro* drug release and *in vivo* results suggest that RST_{30} is the best batch. The above study indicates that the oral bioavailability of RG can be enhanced by formulating it into SLN. Furthermore, SLN developed from a binary lipid matrix showed more promising *in vitro* and *in vivo* results than single lipid core materials and thus may be used as a suitable carrier system for oral delivery of RG.

Table 5. Pharmacodynamic Parameters of the Repaglinide in Diabetic Rats

Preparation	AUEC (% h)	Nadir Effect (%)	T_{Nadir} (h)
RG suspension (control)	49.409 ± 3.45	62.53 ± 2.19	0.3
RSA	1233.201 ± 2.6^{b}	59.66 ± 3.85	4^{b}
RST_{30}	$1476.98 \pm 3.98^{a,b}$	$67.82 \pm 2.14^{a,b}$	$4^{\dagger\dagger b}$

[a] Statistical significance with RSA, $p < 0.05$.
[b] Statistical significance with RG suspension, $p < 0.05$.

CONCLUSION

The present investigation demonstrates that the admixture of TS in the nanoparticle formation process is a feasible approach for the modification of the inner structure of SA (fatty acid) based nanoparticles. This modification may have a consequence in the EE of these structures as well as in their storage stability. It is confirmed from the extensive studies that TS disrupt the crystallinity of the fatty acid (SA). The disorders in crystalline structure provide space to accommodate the RG; this may provide help to increase the EE with excellent physical stability of SLN. Furthermore, pharmacodynamic and pharmacokinetic studies show the potential therapeutic efficacy of RG–SLN in diabetic-induced rats. A much higher bioavailability of RG may be achieved successfully with binary lipid based carrier system. The present work opens new possibility of successful utilization of binary lipid matrix as a carrier for delivery of water insoluble drug(s).

PROSPECTIVE

The binary lipid matrix based SLNs demonstrate high RG encapsulation and good physical stability. A much higher bioavailability of RG was achieved successfully with binary lipid based carrier system in diabetic-induced rats. This work can be extended to other bioactive molecules and vaccine for improving their bioavailability. The new lipid carrier will definitely offer edge over others for oral bioavailability enhancement of water insoluble drugs. The MTT cell lines assay ((3-(4, 5-dimethylthiazol- 2-yl)-2, 5-diphenyl-tetrazolium bromide) will be carried out in the future to confirm the safety level of RG–SLNs in diabetic-induced rats.

ACKNOWLEDGMENTS

We acknowledge the help of Prof. O. N. Srivastava, Department of Physics, Prof. G. Singh and Dr. Madhu Yashpal, Department of Anatomy, Institute of Medical Sciences, Banaras Hindu University, Varanasi, India, in carrying TEM and ED analysis of solid lipid nanoparticles. We also acknowledge the University Grant Commission (UGC), India for providing the financial support in the form of the Senior Research Fellowship.

Table 6. Pharmacokinetic Parameters of the Repaglinide in Diabetic Rats

Parameters	RG Suspension	RSA	RST_{30}
T_{max} (h)	0.300	4.00^{b}	4.00^{b}
C_{max} (ng/mL)	8.50 ± 0.01	9.65 ± 0.045	8.81 ± 0.089
K (h^{-1})	0.66 ± 0.040	0.117 ± 0.09^{b}	$0.064 \pm 0.098^{a,b}$
$t_{1/2}$ (h)	1.05 ± 0.24	5.91 ± 0.61^{b}	$10.89 \pm 0.230^{a,b}$
AUC (h × ng/mL)	8.08 ± 1.98	88.37 ± 2.01^{b}	$109.57 \pm 3.01^{a,b}$
MRT (h)	1.52 ± 0.67	8.53 ± 0.07^{b}	15.71 ± 0.10^{b}
% FFr	100	1093.69 ± 2.56^{b}	$1356.06 \pm 3.03^{a,b}$

[a] Statistical significance with RSA, $p < 0.05$.
[b] Statistical significance with RG suspension, $p < 0.05$.

REFERENCES

1. O'Driscoll CM. 2002. Lipid-based formulations for intestinal lymphatic delivery. Eur J Pharm Sci **15**:405–415.
2. Bargoni R, Cavalli O, Caputo A, Fundaro MR, Gasco, Zara GP. 1998. Solid lipid nanoparticles in lymph and plasma after duodenal administration to rats. Pharm Res **15**:745–750.
3. Vyas SP, Jaitely V, Kanaujia P. 1999. Synthesis and characterization of palmitoyl propranolol hydrochloride auto-lymphotrophs for oral administration. Int J Pharm **186**:177–189.
4. Muhlen AZ, Mehnert W. 1998. Drug release and release mechanism of prednisolone loaded solid lipid nanoparticles. Pharmazie **53**:2–55.
5. Porter CJ, Charman WN. 2001. *In vitro* assessment of oral lipid based formulations. Adv Drug Deliv Rev **50**:S127–S147.
6. Hussain N, Jaitley V, Florence AT. 2001. Recent advances in the understanding of uptake of microparticulate across the gastrointestinal lymphatics. Adv Drug Deliv Rev **50**:107–142.
7. Sarmento B, Susana M, Domingos F, Eliana SB. 2007. Oral insulin delivery by means of solid lipid nanoparticles. Int J Nanomed **2**:743–749.
8. Zara GP, Bargoni A, Cavalli R, Fundaro A, Vighetto D, Gasco MR. 2002. Pharmacokinetics and tissue distribution of idarubicin-loaded solid lipid nanoparticles after duodenal administration to rats. J Pharm Sci **91**:1324–1333.
9. Manjunath K, Venkateswarlu V. 2006. Pharmacokinetics, tissue distribution, and bioavailability of nitrendipine solid lipid nanoparticles after intravenous and intraduodenal administration. J Drug Target **14**:632–645.
10. Paliwal R, Rai S, Vaidya B, Khatri K, Goyal AK, Mishra N, Mehta A, Vyas SP. 2009. Effect of lipid core material on characteristics of solid lipid nanoparticles designed for oral lymphatic delivery. Nanomedicine **5**:184–191.
11. Luo YF, Chen DW, Ren LX. 2006. Solid lipid nanoparticles for enhancing vinpocetine's oral bioavailability. J Control Release **114**:53–59.
12. Li H, Zhao X, Ma Y, Zhai G, Li L, Lou H. 2009. Enhancement of gastrointestinal absorption of quercetin by solid lipid nanoparticles. J Control Release **133**:238–244.
13. Mehnert W, Mader K. 2001. Solid lipid nanoparticles: production, characterization and applications. Adv Drug Deliv Rev **47**:165–196.
14. Manjunath K, Reddy JS, Venkateswarlu V. 2005. Solid lipid nanoparticles as drug delivery systems. Methods Find Exp Clin Pharmacol 27:127–144.
15. Windbergs M, Strachan CJ, Kleinebudde P. 2009. Understanding the solid-state behaviour of triglyceride solid lipid extrudates and its influence on dissolution. Eur J Pharm Biopharm 71:80–87.
16. Jenning V, Gohla S. 2000. Comparison of wax and glycerides solid lipid nanoparticles. Int J Pharm 196:219–222.
17. Mayer-Davis EJ, Levin S, Bergman RN. 2001. Insulin secretion, obesity, and potential behavioral influences: results from the Insulin Resistance Atherosclerosis Study (IRAS). Diabetes Metab Res Rev 17:137–145.
18. Muthu MS, Singh S. 2008. Studies on biodegradable polymeric nanoparticles of risperidone: *In vitro* and *in vivo* evaluation. Nanomedicine 2:233–240.
19. US. Pharmacopeia. XXIV, 2006. Vol. USP 29. Rockville, MD.
20. Holm R, Mullertz A, Christensen E, Hoy CE. 2001. Comparison of total oral bioavailability and the lymphatic transport of halofantrine from three different unsaturated triglycerides in lymph-cannulated conscious rats. Eur J Pharm Sci **14**:331–337.
21. Verger ML, Fluckiger L, Kim Y. 1998. Preparation and characterization of nanoparticles containing an antihypertensive agent. Eur J Pharm Biopharm 46:137–143.
22. Singh S, Muthu MS. 2007. Preparation and characterization of nanoparticles containing an atypical antipsychotic agent. Nanomedicine 3:305–319.
23. Moneghini M, Volinovich D, Princivalle F. 2000. Formulation and evaluation of vinypyrrolidone/vinylacetate copolymer microspheres with carbamazepine. Pharm Dev Technol 5:347–353.
24. Kim A, Yun MO, Oh YK, Ahn WS, Kim CK. 1999. Pharmacodynamics of insulin in polyethylene glycol-coated liposomes. Int J Pharm 180:75–81.
25. Lu Y, Zhang Y, Yang Z, Tang X. 2009. Formulation of an intravenous emulsion loaded with clarithromycin-phospholipid complex and its pharmacokinetics in rats. Int J Pharm 366:160–169.
26. Goldberg IJ, Isaacsa A, Sehayekb E, Breslowb JL, Huanga LS. 2004. Effects of streptozotocin-induced diabetes in apolipoprotein AI deficient mice. Atherosclerosis 172:47–53.
27. Adikwu MU, Yoshikawa Y, Takada K. 2004. Pharmacodynamic-pharmacokinetic profiles of metformin hydrochloride from a mucoadhesive formulation of a polysaccharide with antidiabetic property in streptozotocin-induced diabetic rat models. Biomaterials 25:3041–3048.
28. Bunjes H, Westesen K, Koch MHJ. 1996. Crystallization tendency and polymorphic transitions in triglyceride nanoparticles. Int J Pharm 129:159–173.
29. Jenning V, Thunemann AF, Gohla SH. 2000. Characterisation of a novel solid lipid nanoparticle carrier system based on binary mixtures of liquid and solid lipids. Int J Pharm 199:167–177.
30. Westesen K, Bunjes H, Koch MJH 1997. Physicochemical characterization of lipid nanoparticles and evaluation of their drug loading capacity and sustained release potential. J Control Release 48: 223–236.
31. Gisele A, Castro Lucas A, Ferreira M. 2008. Characterization of a new solid lipid nanoparticle formulation containing retinoic acid for topical treatment of acne. Powder Diffr 23:S31–S35.

32. Olbrich C, Muller RH. 1999. Enzymatic degradation of SLN—effect of surfactant and surfactant mixtures. Int J Pharm 180:31–39.
33. Garcia-Fuentes M, Torres D, Alonso MJ. 2003. Design of lipid nanoparticles for the oral delivery of hydrophilic macromolecules. Colloid Surf B Biointerfaces 27:159–68.
34. Roger E, Lagarce F, Benoit JP. 2009. The gastrointestinal stability of lipid nanocapsules. Int J Pharm 379:260–265.
35. Muller RH, Mader K, Gohla S. 2000. Solid lipid nanoparticles (SLN) for controlled drug delivery–A review of the state of the art. Eur J Pharm Biopharm 50:161–177.
36. Wissing SA, Kayser O, Muller RH. 2004. Solid lipid nanoparticles for parenteral drug delivery. Adv Drug Deliv Rev 56:1257–1272.
37. Kumar VV, Chandrasekar D, Ramakrishna S. 2007. Development and evaluation of nitrendipine loaded solid lipid nanoparticles: Influence of wax and glycerid lipids on plasma pharmacokinetics. Int J Pharm 335:167–175.
38. Hu FQ, Jiang SP, Du YZ. 2005. Preparation and characterization of stearic acid nanostructured lipid carriers by solvent diffusion method in an aqueous system. Colloids Surf B Biointerfaces 45:167–173.
39. Betancourt T, Brown B, Brannon-Peppas L. 2007. Doxorubicin–loaded PLGA nanoparticles by nanoprecipitation: Preparation, characterization and in vitro evaluation. Nanomedicine 2:219–232.
40. Mansbach CM, Nevin P. 1998. Intracellular movement of triacylglycerols in intestine. J Lipid Res 39:963–968.
41. Cavalli R, Bargoni A, Podio V, Muntoni E. 2003. Duodenal administration of solid lipid nanoparticles loaded with different percentages of tobramycin. J Pharm Sci 92:1085–1094.
42. Nordskog BK, Phan CT, Nutting DF, Tso P. 2001. An examination of the factors affecting intestinal lymphatic transport of dietary lipids. Adv Drug Deliv Rev 50:21–44.
43. Ros E. 2000. Intestinal absorption of triglyceride and cholesterol, dietary and pharmacological inhibition to reduce cardiovascular risk. Atherosclerosis 151:357–379.
44. Mullar RH, Runge S, Ravelli V, Mehnert W, Thunemann AF, Souto, EB. 2006.Oral bioavailability of cyclosporine: Solid lipid nanoparticles (SLN) versus drug nanocrystals. Int J Pharm 317:82–89.